Since January 2020 Elsevier has created a COVID-19 resource centre with free information in English and Mandarin on the novel coronavirus COVID-19. The COVID-19 resource centre is hosted on Elsevier Connect, the company's public news and information website.

Elsevier hereby grants permission to make all its COVID-19-related research that is available on the COVID-19 resource centre - including this research content - immediately available in PubMed Central and other publicly funded repositories, such as the WHO COVID database with rights for unrestricted research re-use and analyses in any form or by any means with acknowledgement of the original source. These permissions are granted for free by Elsevier for as long as the COVID-19 resource centre remains active.

Materials Today: Proceedings 49 (2022) 2999–3007

Contents lists available at ScienceDirect

Materials Today: Proceedings

journal homepage: www.elsevier.com/locate/matpr

Molecular docking and ADMET study of bioactive compounds of *Glycyrrhiza glabra* against main protease of SARS-CoV2

Vivek Srivastava [a,*], Ankush Yadav [b], Paratpar Sarkar [a]

[a] Department of Chemistry and Biochemistry, School of Basic Sciences and Research, Sharda University, Greater Noida-201308, UP, India
[b] Department of Biochemistry, School of Chemical and Life Sciences, Jamia Hamdard, New Delhi 110062, India

ARTICLE INFO

Article history:
Received 1 September 2020
Accepted 3 October 2020
Available online 14 October 2020

Keywords:
Main protease (M^{pro})
Glycyrrhiza glabra
SARS-CoV2
Molecular docking
ADMET

ABSTRACT

Recent pandemic situation of COVID-19 is caused due to SARS-CoV2 and almost all the countries of the world have been affected by this highly contagious virus. Main protease (M^{pro}) of this virus is a highly attractive drug target among various other enzymes due to its ability to process poly-protein that is the translated product of the SARS-CoV2 RNA. The present study demonstrates molecular docking study of *Glycyrrhiza glabra (Gg)* active compounds such as Glycyrrhizic acid (GA), Liquiritigenin (L) and Glabridin (G) against the M^{pro}. Docking studies shows that these active compounds bind strongly with some of the amino acid residues in the active site of M^{pro} and inhibits the enzyme strongly. GA, L, and G are proposed to be strong inhibitors of the enzyme and the amino acids: His^{41}, Gly^{143}, Gln^{189}, Glu ^{166}, Cys ^{145}, Thr^{25}, Asn^{142}, Met^{49}, Cys^{44}, Thr^{45} and pro^{168} present in the active site of M^{pro} were shown to make non-covalent interaction with these compounds. In silico ADMET properties prediction also shows that *Gg* active compounds had good solubility, absorption, permeation, non-toxic, and non– carcinogenic characteristics. Our finding concludes that all of the three active compounds of *Gg* have the potential to be strong inhibitors for M^{pro} of SARS-CoV2 but glycyrrhizic acid has a high binding affinity and a good ADMET properties than the other two.
© 2020 Elsevier Ltd. All rights reserved.
Selection and peer-review under responsibility of the scientific committee of the National Conference on Functional Materials: Emerging Technologies and Applications in Materials Science.

1. Introduction

Wuhan, Hubei province of China was the very first location where the severe acute respiratory syndrome coronavirus2 (SARS-CoV2) outbreak recorded [1]. From Wuhan city of China this virus had spread across more than 200 countries with America and Brazil as the epicentre as of now. COVID-19 caused by SARS-CoV2 has affected 8, 242, 999 people worldwide and killed as many as 445, 535 people, global data as of 18th June 2020, 4.57 pm CEST. (WHO coronavirus disease Dashboard). World Health Organization (WHO) has stated the COVID-19, a public health emergency of international concern on January 30, 2020 [2]. SARS-CoV [3], MERS-CoV [4] and SARS-CoV2 [5] are the three categories of coronavirus that causes the deadly pneumonia in humans. Severe acute respiratory syndrome-2 (SARS-CoV2) is an enveloped, positive-sense single-strand RNA placed in a beta coronavirus family of *Coronaviridae* [6]. As compared to the other two, SARS-CoV2 is highly contagious and spread the infection more quickly and severely, leading to large number of deaths and thus arising a pandemic situation [7,8].

The SARS-CoV2 has a genome ranging from 29 to 30 kb in length [9]. The recently proposed drugs targets the main protease (M^{pro} also known as $3CL^{pro}$) which is one of the best targets among the other enzymes in the virus [10]. This enzyme participates in the processing of polyprotein that is translated from the RNA of the same virus [11]. These polyprotein are processed and converted into mature non-structural proteins using two proteases PL^{pro} and CL^{pro} encoded by ORF1 (open reading frame1) [12]. A non-structural protein of coronavirus plays a significant role in replication and transcription during the infection [13]. Main protease operates at more than 10 cleavage sites on the polyprotein 1ab which is nearly 790 kDa [14]. M^{pro} is a homodimer having two identical chains and the recognition sequence is Leu-Gln ↓ Ser, Ala, Gly and cleaved through the Cys-His dyad protease in which -SH group of cysteine serve as a nucleophile in the proteolysis [15]. Inhibiting the main protease activity would block transcription or replication. The amino acid residues of the active site

* Corresponding author.
E-mail address: vivek.srivastava1@sharda.ac.in (V. Srivastava).

https://doi.org/10.1016/j.matpr.2020.10.055
2214-7853/© 2020 Elsevier Ltd. All rights reserved.
Selection and peer-review under responsibility of the scientific committee of the National Conference on Functional Materials: Emerging Technologies and Applications in Materials Science.

of M^{pro} participating in substrate binding includes Cys145 –His41 dyad ,and Phe140, Thr45, Arg188, Asp187, Met49, Asn142, Met165, Gln189, His172, Glu166 [16]. An enormous amount of data is available for describing the efficiency of an array of various active components of medicinal plants effective against the viruses. Among these medicinal plant, *Glycyrrhiza glabra* is the one plant, its active compounds may have the potential to act against various viruses [17]. *Glycyrrhiza glabra (Gg)* commonly called 'sweet wood' and 'liquorice' belongs to the family Fabaceae. It has been effective against many RNA viruses like H5N1virus, Hepatitis C virus, influenza A virus, Newcastle disease virus, H1N1 virus, Rotavirus, severe acute respiratory virus etc. and DNA viruses such as Varicella Zoster virus, Epstein-Barr virus and Herpes Simplex virus etc. [18].

Several active compounds from *Gg* have been reported that inhibit the virus's growth. Some studies showed that Glycyrrhizin (glycyrrhizinate; glycyrrhizic acid) inhibit the binding of the virus to the target cells, and also beneficial in controlling the viral replication and found to have an important antiviral activity. Studies on clinically isolates of severe acute respiratory syndrome Virus [FFM-1 and FFM-2] gave important information about the anti-viral property of glycyrrhizic acid [19,20]. Another active compound, Glabridin (G) isolated from *Gg* roots. It has been used as a traditional medicine in Asia and has anti-inflammatory, anti-osteoporotic, anti-nephritic, anti-antheroenic, estrogenic, and anti-oxidant, regulation of metabolism, neuro-protective and skin-whitening properties. This is also reported to have vasodilation property and used for the treatment of many diseases like bacterial, bronchitis infection [27,28]. Liquiritigenin (L) has anti-cancer, anti-oxidative, antimicrobial activities, hepato-protective, immune regulatory, and cardio-protective effects and also has anti-platelet aggregation, anti-tumorigenic, anti-angiogenic, anti-allergic properties [29].

For the virtual screening and structure-based drug designing, molecular docking is commonly used in bioinformatics based research and is accustomed to predict non-covalent interaction (mainly hydrogen bonding) of macromolecule (receptor) with the ligand (drug molecule). AutoDock is a suited program for docking and virtual screening which calculates the grid internally (automatically), for the atom types that are required. A more improved version, AutoDock Vina achieves within the average accuracy of the binding pose prediction and bring order of magnitude faster than previously developed AutoDock4 [30].

OSIRIS Property Explorer is employed to determine drug Likeness. It provides drug relevant information whenever a structure is valid and underlines various properties with a high risk of inadmissible effects such as poor intestinal absorption, mutagenicity or drug conform behaviour through different customization characteristics. This also determines the clog P (Logarithm of compounds partition coefficient between water and n-Octanol) which determines the hydrophilicity of the compounds. Larger the clogP value, lower the hydrophilicity and thus poor the permeation and absorption. Log S suggest solubility; lower the log S value, higher the solubility which enhances the absorption. The Topological polar surface area (TPSA) suggest the surfaces that belong to the polar atoms and molecules in the compound. Larger TPSA value is related with the least permeability of the membrane. The compounds that have larger TPSA value will be a better substrate for p-glycoprotein which is liable for efflux of drug from the cell and thus reduced TPSA was beneficial for drug-like property. Some studies also anticipated that a molecule having a better penetration property through CNS should have lesser value of TPSA [26].

A good drug candidate can be consumed in the desired time as well as distributed through the entire body for its efficient action and metabolism. Another factor is toxicity which is often very vital and dominates the Absorption, Distribution, Metabolism, Excretion behaviour of the drugs. Some studies have shown that drug failed at clinical trials due to its adverse side effect and their toxicity which has been proven to be very detrimental and expensive in the drug development. In silico, ADMET and drug-likeness prediction help in the discovery of new targets and compounds with anticipated biological activities [31]. Human intestinal absorption [HIA] is an important ADMET properties. The exploitation of drugs in the body is such a complex process that can hardly analysed by statistical models. HIA is one of the important steps during compounds (drug) transporting to their desired target [31]. Blood-brain barrier [BBB] is used to predict various features of the CNS vasculature. CNS vessel does not have pores in the endothelial cell and have various properties that regulate the transport of ions, molecules, and cells which make CNS vessel very prohibitive in nature and provides an interference for the delivery of compounds into the central nervous system [32]. Carcinogenicity means the ability of the substance to cause cancer. P-glycoprotein substrate is a compound that utilizes the P-glycoprotein transporter for several exercises like excretion and absorption of drugs and other vital exercises [33]. These properties are often used for the study of ADMET behaviour of the drugs.

The main objective of the present study is to carry out molecular docking analysis of *Glycyrrhiza glabra* active compounds, Glycyrrhizic acid, Liquiritigenin and Glabridin against the main protease (M^{pro}) one by one followed by molecular interaction study (hydrogen bond prediction between target and drugs), drug-likeness behaviour and ADMET prediction to confirm the efficiency and efficacy of these active compound against SARS-CoV2.

2. Methods and materials

2.1. Selection of ligand

Glycyrrhizic acid (PubChem CID: 14982), Liquiritigenin (PubChem CID: 114829), and Glabridin (PubChem CID: 124052) were recognized as potential SARS-CoV inhibitors from literature survey and maybe also effective against SARS-CoV2. The structure of Liquiritigenin and Glabridin, and Glycyrrhizic acid were downloaded from PubChem (http://pubchem.ncbi.nlm.nih.gov) two control drug that is lopinavir (PubChem CID: 92727) and rotinavir (PubChem CID: 39622) also downloaded and converted their file format from SDF file to PDB file [Supplementary Fig. 1 (a) – (c)].

2.2. Selection of target molecule (Receptor/M^{pro}): Active site and sequence analysis

The crystal structure of the main protease (PDB ID- 6Y2E) downloaded from PDB database https://www.rcsb.org/structure/6Y2E, DOI: https://doi.org//10.2210/pdb6Y2E/pdb [25] and saved as PDB format. Its functional domain and the number and name of amino acid residues present in the pocket of the active site of 6Y2E were verified using ScanProsite (ExPASy) (http://prosite.expas.org) (supplementary figure S4) [21] and CDD webserver was used to determine the conserved sequence of 6Y2E [22], Sequence analysis of the main protease of SARS-CoV2 was retrieved using ProtParam, ProtScale (http://web.expasy.org) [23].

2.3. Preparation of ligands (Glycyrrhiza glabra active compounds) and main protease (M^{pro})

The Ligand was prepared by adjusting ionization, torsion, degree of freedom and stereo-chemical variation using AutoDock MG Tool. Energy of the main protease was minimized based on GROMAS6 43B1 algorithm using Swiss Model Viewer, water was removed and Polar hydrogens were added to the main protease

of SARS-CoV2 followed by calculation of gasteiger Charges using the AutoDock MG Tool and saved in PDBQT file format. The receptor grid was developed using AutoDock Grid tool with grid dimensions of $30A^0 \times 30A^0 \times 30$ A^0 with 0.375 A^0 spacing and the grid box was set at −15.692, −32.457, 2.498 in X, Y and Z dimension [24].

2.4. Molecular docking of Glycyrrhiza glabra (Gg) active compounds with M^{pro}

The crystal structure main protease (M^{pro}) downloaded from RCSB Protein Data Bank (PDB ID: 6Y2E) with a resolution of 1.7 A^0 and R-value free of 0.222 and R-value work of 0.171. Molecular docking was performed using in silico docking software, AutoDock Vina [30] with the three active compounds of *Gg*, glycyrrhizic acid, liquiritigenin and glabridin one by one against 6Y2E. The docking was done using command Prompt and the other prerequisite conditions before the docking like the ligand and enzyme preparation has been established. PyMol and BIOVIA Discovery Studio Visualizer was used to visualize the binding interaction between the active compounds of *Glycyrrhiza glabra* with 3D structure of M^{pro} (6Y2E) of SARS-CoV2 [25] and Simulation was done with CHARMM36 force field in Discovery Studio visualisation tool.

2.5. Drug likeness prediction

OSIRIS Property Explorer (http://www.organic-chemistry.org/prog/peo/) [26] is employed to determine likeness of drugs. Properties like Log S calculation, TPSA, Clog P calculation, molecular mass, and drug-likeness based on fragment and drug score of all the three active compounds have been established.

2.6. ADMET properties prediction

ADMET refers to Absorption, Distribution, Metabolism, Excretion, and Toxicity. It contains the pharmacokinetic profile of a compound (drug molecule) and plays a significant role in determining its pharmacodynamics activities. Taking all the three active compounds into account, properties like bioavailability, brain penetration, oral absorption, carcinogenicity, and other human intestinal absorption properties of the active compounds have been deter-

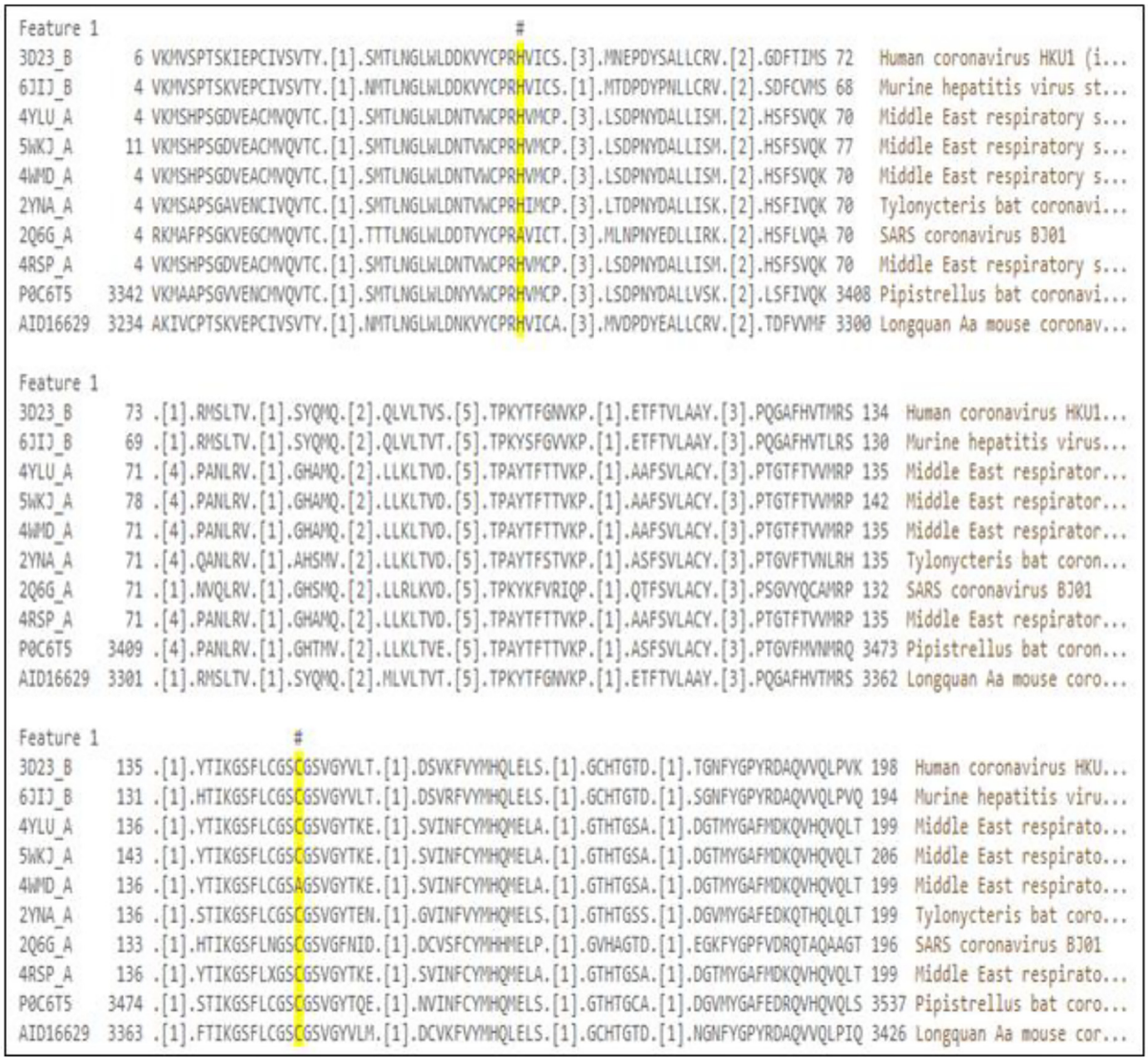

Fig 1. Sequence alignment using CDD webserver represent His^{41} and Cys^{145} as highly conserved amino acids (denoted by #) in all coronaviruses and actively participated in cleavage of polyprotein of SARS-CoV2 into structural proteins.

mined using admetSAR webserver (http://Immd.ecust.edu.cn:8000/) [31–34].

3. Results and discussion

3.1. Sequence analysis and active site identification

Sequence analysis of SARS-CoV2 M^{pro} revealed a theoretical PI value of 5.95 with an extinction coefficient of 33640 M^{-1} cm^{-1} and absorbance (1 g/L) computed 0.995. The Aliphatic index of the M^{pro} was 82.12 and shows a stability index of 27.65. All these result shows that SARS-CoV2 M^{pro} is a very stable macromolecule. The secondary structure of SARS-CoV2 main protease revealed that the alpha helix and the beta strand were maximally present (supplementary table 1). The ExPASy Prosite and CDD webserver result shows that His^{41} and Cys^{145} has a vital role in the catalytic activity of the main protease of SARS-CoV2 and also has been conserved in all the different types of coronaviruses as depicted in Fig. 1.

3.2. Molecular docking analysis of control drugs with the M^{pro} of the SARS-CoV2

The molecular docked pose of the minimum binding affinity conformer of the Lopinavir and Ritonavir (control drugs) demonstrated that they bind to the active site of the M^{pro} protein of the SARS-CoV2. Fig. 2 showed that Lopinavir binds through two conventional H-bond with Asn^{142}, two carbon H-bond with Thr^{25} and Gln^{189}, and two alkyl bond with His^{41} respectively. However, Ritonavir also bind firmly to the active site of the main protease and it stabilized the M^{pro} active site through four hydrogen Bond in which two are conventional hydrogen bond and rest two are carbon hydrogen bond. Asn^{142} and Thr^{25} amino acid residue formed conventional and carbon hydrogen bond respectively. Whereas Cys^{44} and Cys^{145} formed alkyl bond and His^{41} and Pro^{168} shows Pi-alkyl interaction, besides other residues also found to be bound to control drugs through Vander Waals interaction depicted in 2D (two dimensional) plot (Fig. 3). The binding affinity energy of the control drugs are mentioned in table 1. If we compare the binding affinity energy of control drugs, Lopinavir and Ritonavir, we observed that Lopinavir have highest negative binding affinity with −7.6 Kcal/mol followed by Ritonavir with −7.3 Kcal/mol [35].

3.3. Molecular docking analysis of Gg active compounds with the M^{pro} of the SARS-CoV2

The molecular docked pose of the minimum binding affinity conformer of the Gg active compounds that is glycyrrhizic acid, Glabridin and Liquiritigenin demonstrated that they also firmly goes and bind to the active site of the M^{pro} protein of the SARS-CoV-2 (Fig. 4 and table 2). Glycyrrhizic acid (GA) binds within the M^{pro} active site through several non-covalent interactions. GA binds active site through one conventional H-bond with Glu^{166} and three carbon H-bond with Ser^{46}, Pro^{168} and Asn^{142}. GA also found to be bound to active site through alkyl and Pi-alkyl bond with Cys^{145}, Leu^{27} and His^{41} respectively (Fig. 7). Glabridin stabilizes the M^{pro} active site through hydrogen bond with His^{41} and Glu^{166} and through alkyl and Pi-alkyl with Cys^{145} and Pro^{168} respectively and play an important role in the stabilisation of the active site of the main protease (Fig. 6). Likewise Liquiritigenin also binds to the active site and formed several non-covalent interaction in which Thr^{25} and Thr^{45} are found to bind with the Liquiritigenin through hydrogen bond and, Met^{49}, and Cys^{145} formed Pi-sulfur interaction to Liquiritigenin L also firmly binds to the His^{41} through Pi-Alkyl that stabilize the active site (Fig. 5). On comparing the binding affinity of the control drugs with the binding affinity of Gg active compounds, we found that GA have the highest negative binding affinity energy than Lopinavir and ritonavir with −8.0 Kcal/mol, G have lower binding affinity than Lopinavir but have similar binding affinity with ritonavir with −7.3 Kcal/mol whereas L have lowest binding affinity among all ligands [36].

3.4. Drug likeness prediction

The result of the OSIRIS Property Explorer (http://www.organic-chemistry.org/prog/peo/) shown in table 3. Out of the three active compounds, GA shows a very low Clog P than G and L and thus GA

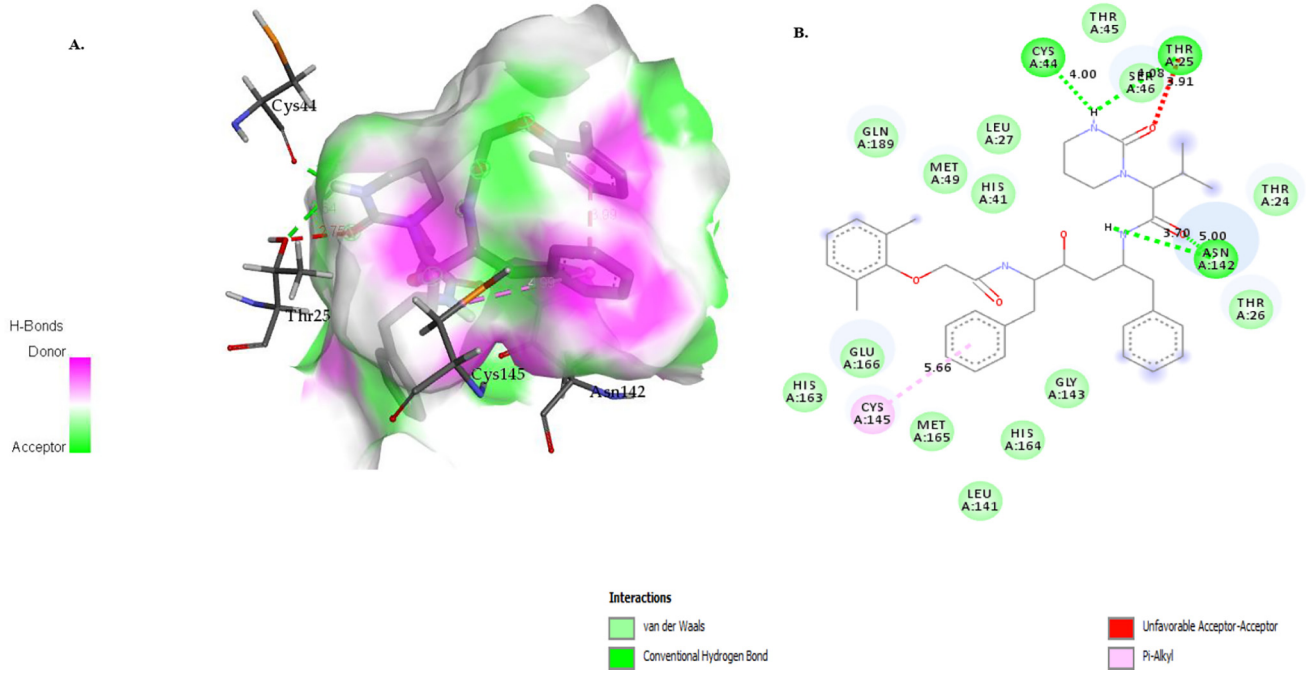

Fig. 2. 3-D (three-dimensional) diagram based on hydrogen bond donor and acceptor characteristics of amino acid residues (A) and 2-D (two dimensional) (B) diagram showing several interaction between M^{pro} and Lopinavir. CYS: Cysteine, THR: Threonine, ASN: Asparagine.

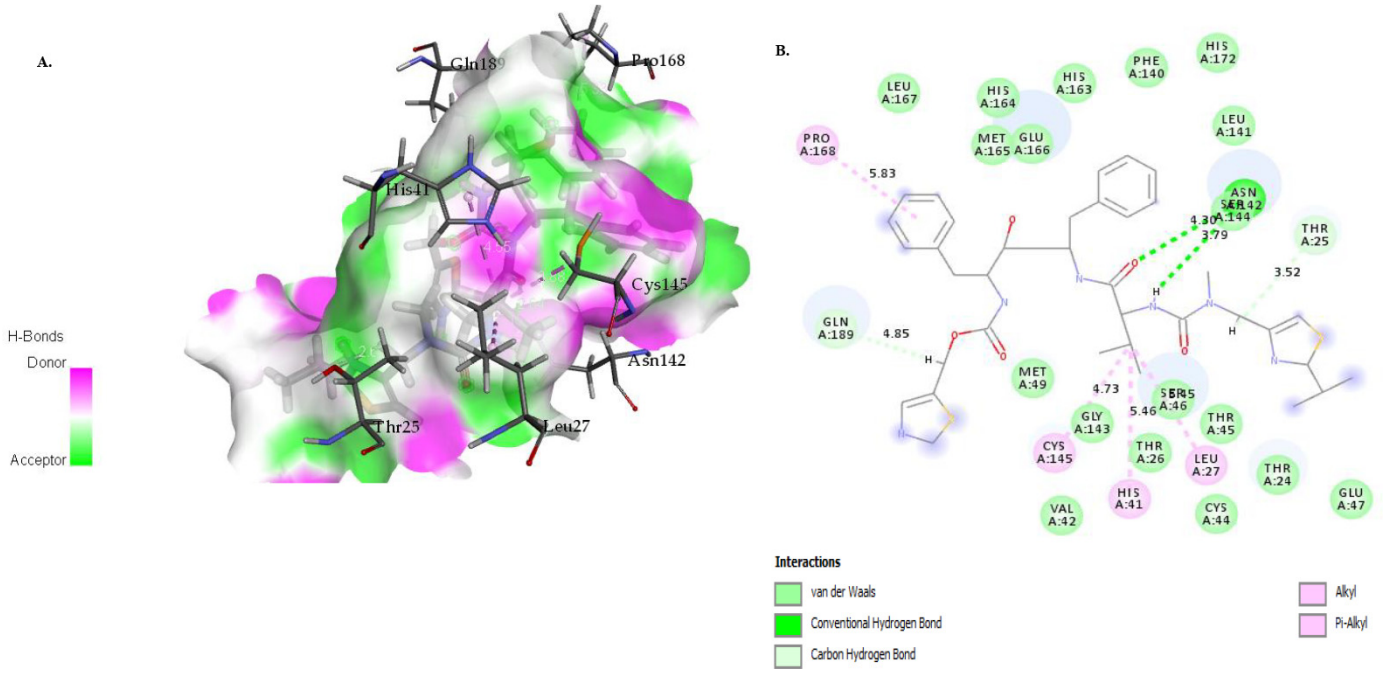

Fig. 3. 3-D (three dimensional) diagram based on hydrogen bond donor and acceptor characteristics of amino acid residues (A) and 2-D (two dimensional) (B) diagram showing several interaction between M^{pro} and Ritonavir. PRO: Proline, THR: Threonine, LEU: Leucine, HIS: Histidine, ASN: Asparagine.

Table 1
Molecular Docking analysis: Binding energy and the type of molecular interaction of control drugs against M^{pro}. UNK: *Glycyrrhiza glabra* active compounds.

Control Drugs	Binding Affinity (Kcal/mol)	Donor Atom	Distance	Acceptor Atom	Category	Types of interaction
Lopinavir	−7.6	ASN142:HD22	2.39	UNK: O	Hydrogen Bond	Conventional H-bond
		UNK:H	1.75	ASN142:OD1	Hydrogen Bond	Conventional H-bond
		UNK:H	2.63	THR25:OG1	Hydrogen Bond	Conventional H-bond
		UNK:H	1.72	CYS44	Hydrogen Bond	Conventional H-bond
		UNK	3.98	UNK	Hydrophobic	Pi-Pi Stacked
		UNK	4.98	CYS145	Hydrophobic	Pi-Alkyl
Ritonavir	−7.3	ASN142:HD22	2.63	UNK: O	Hydrogen Bond	Conventional H-bond
		UNK:H1	2.43	ASN142:OD1	Hydrogen Bond	Conventional H-bond
		UNK:H13	2.61	THR25:OG1	Hydrogen Bond	Carbon H-bond
		UNK:H34	2.23	GLN189:OE1	Hydrogen Bond	Carbon H-bond
		UNK:C12	5.14	LEU27	Hydrophobic	Alkyl
		UNK:C12	3.87	CYS145	Hydrophobic	Alkyl
		HIS41	4.55	UNK:C12	Hydrophobic	Pi-Alkyl
		UNK	5.33	PRO168	Hydrophobic	Pi-Alkyl

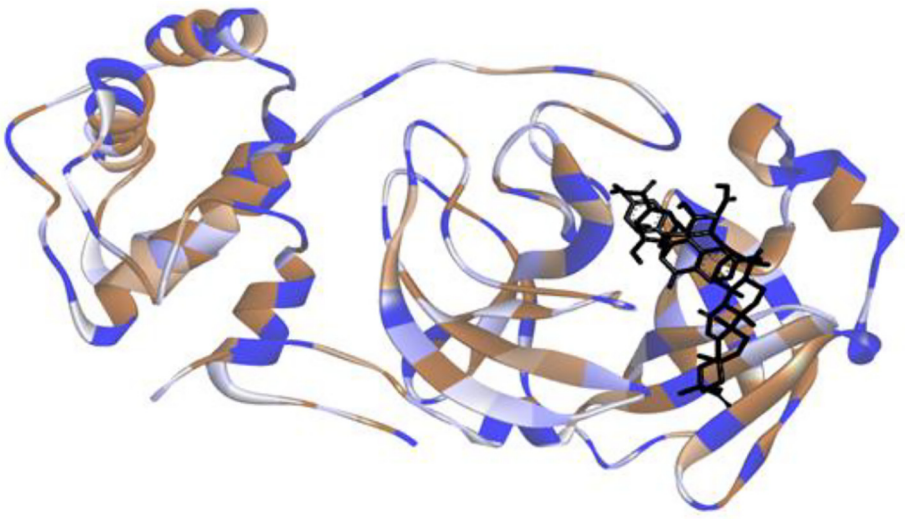

Fig 4. Three dimensional structure of main Protease based on the hydrophobicity of amino acid residues and docked compounds are shown in black.

has high hydrophilicity and can be absorbed easily by the cell of the SARS-CoV2 thus showing drug efficacy but in terms of solubility, GA is least soluble in blood than the other two. L shows maximum solubility in the blood. TPSA of GA is also higher as compared with the other two compounds which tell the efficiency of the compounds in terms of membrane permeability. Here again GA has more potential to cross the lipid bilayer of the virus and thus can strongly bind and inhibits the enzyme (M^{pro}). Our predicted values lie well within the drug-likeness.

3.5. ADMET prediction

ADMET (Absorption, Distribution, Metabolism, Excretion and Toxicity) properties were retrieved using admetSAR server, which shows that all *Glycyrrhiza glabra* active compounds i.e. Glycyrrhizic acid (GA) (Accession Number: DB13751), Liquiritigenin (L) (PubChem CID: 114829) and Glabridin (G) (PubChem CID: 124052) are having better human intestinal absorption score (table 4). Higher human intestinal absorption indicates that the compound of interest may be better consumed from the gastrointestinal tract upon oral administration. The penetration through the Blood-Brain Barrier is computed to be the best for G and comparatively higher than L and almost similar to GA. In terms of predicting the efflux by P-glycoprotein from the cell, GA comes out to be inhibitor and non-substrate of P-glycoprotein, G comes out to be non-inhibitor and substrate and L comes out to be non-inhibitor and non-substrate. An inhibitor of P-glycoprotein means that drug will inhibit the efflux process from the cell and enhances the bioavailability and non-inhibitor of P-glycoprotein mean that drug will efflux from the cell by P-glycoprotein and limits the bioavailability by pumping back into the lumen and may promote the elimination of that drug into the bile and urine [34]. In the case of metabolism, GA and G found to be non-inhibitor and substrate while L found to be inhibitor and non-substrate. A non-inhibitor of cytochrome P450 means that the molecule will not hinder the biotransformation of the compound (drug) metabolized by cytochrome P450

Table 2
Molecular Docking analysis: Binding energy and the type of hydrogen bond interaction of all the three active compounds of *Gg* against M^{pro}. UNK: *Glycyrrhiza glabra* active compounds.

Gg active compounds	Binding Affinity (Kcal/mol)	Donor Atom	Distance	Acceptor Atom	Category	Types of interaction
G	−7.3	HIS41:HE2	2.37	UNK:O1	Hydrogen Bond	Conventional H-bond
		UNK:H	1.84	GLU166: O	Hydrogen Bond	Conventional H-bond
		MET49:SD	5.46	UNK	Other	Pi-Sulfur
		CYS145	4.43	UNK	Hydrophobic	Alkyl
		UNK:C12	3.99	CYS145	Hydrophobic	Alkyl
		HIS41	5.34	UNK	Hydrophobic	Pi-Alkyl
		HIS41	5.32	UNK:C12	Hydrophobic	Pi-Alkyl
		UNK	5.2	PRO168	Hydrophobic	Pi-Alkyl
L	−7.0	UNK:H	2.17	THR25: O	Hydrogen Bond	Conventional H-bond
		THR45:H	2.84	UNK:O2	Hydrogen Bond	Carbon H-bond
		MET49:S	5.6	UNK	Other	Pi-Sulfur
		CYS145:S	3.64	UNK	Other	Pi-Sulfur
		HIS41	5.82	UNK	Hydrophobic	Pi-Pi Stacked
GA	−8.0	UNK:H7	2.51	GLU166: O	Hydrogen Bond	Conventional H-Bond
		SER46:HB2	2.47	UNK:O12	Hydrogen Bond	Carbon H-Bond
		PRO168:HD2	2.8	UNK:O14	Hydrogen Bond	Carbon H-Bond
		UNK:H54	2.46	ASN142:OD1	Hydrogen Bond	Carbon H-Bond
		CYS145	5.21	UNK	Hydrophobic	Alkyl
		UNK:C28	5.19	LEU27	Hydrophobic	Alkyl
		HIS41	4.58	UNK:C28	Hydrophobic	Pi-Alkyl

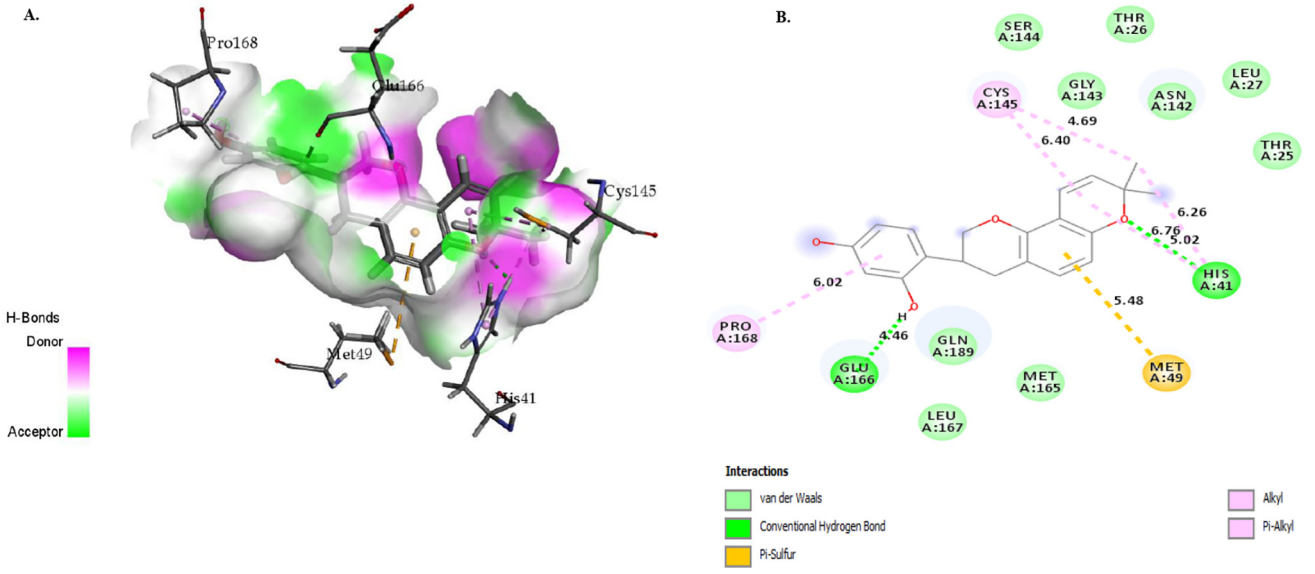

Fig. 6. 3-D (three dimensional) diagram based on hydrogen bond donor and acceptor characteristics of amino acid residues (A) and 2-D (two dimensional) (B) diagram showing several interaction between M^{pro} and Glabridin (G). PRO: Proline, MET: Methionine, GLU: Glutamic acid, CYS: Cysteine, HIS: Histidine.

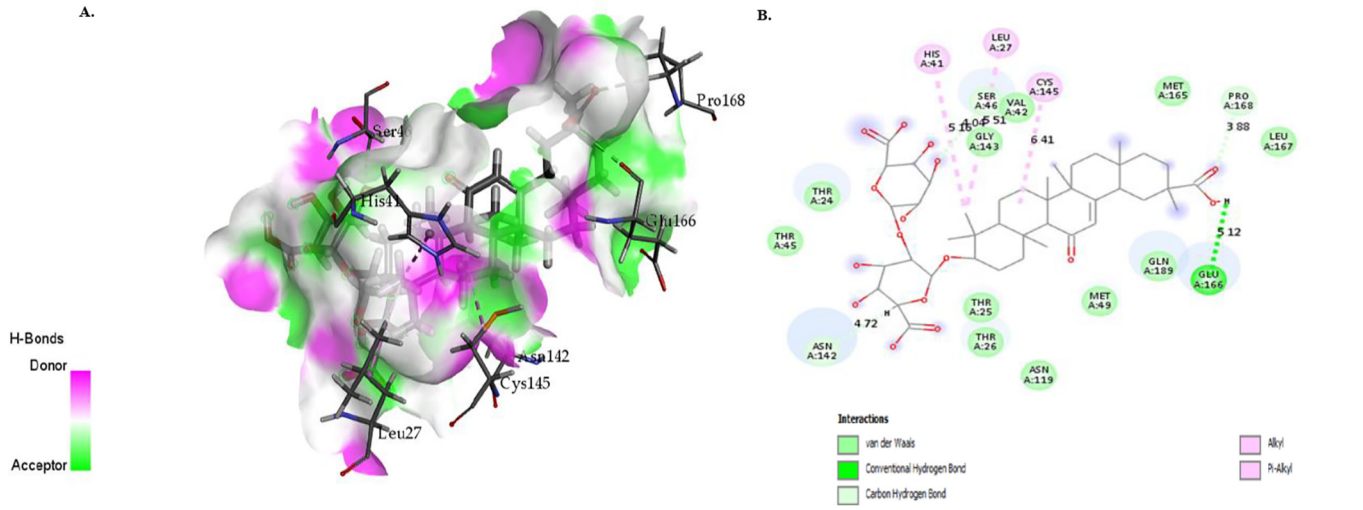

Fig. 7. 3-D (three dimensional) diagram based on hydrogen bond donor and acceptor characteristics of amino acid residues (a) and 2-D (two dimensional) (b) diagram showing several interaction between M^{pro} and Glycyrrhizic acid (GA). HIS: Histidine, GLU: Glutamic acid, LEU: Leucine, ASN: Asparagine, CYS: Cysteine, PRO: Proline.

Table 3
Drug likeness prediction using OSIRIS Property Explorer, clog P (O/W): Logarithm of partition coefficient between n-octanol and water, logS: aqueous solubility, TPSA: Topological polar surface area.

Gg active compounds	clog P(≤5)	Solubility: log S(-6.5 to 0.5)	Molecular mass	TPSA	Overall drug score
GA	0.99	−5.14	822	267	0.19
G	4.31	−4.15	324	58.92	0.24
L	2.5	−2.94	256	66.76	0.42

Table 4
ADMET profile of *Gg* active compounds, HIA: Human intestinal absorption, BBB: Blood Brain Barrier, CYP450: Cytochrome P450.

S.NO	*Gg* active compounds	HIA (probability)	BBB (probability)	Acute oral Toxicity (Kg/mol)	CYP450 3A4 inhibitor/substrate	Carcinogenicity
1.	GA	0.8125	0.8793	2.13283	Non-Inhibitor/substrate	Non carcinogenic
2.	G	0.9948	0.9312	3.11555	Non-Inhibitor/substrate	Non carcinogenic
3.	L	0.9947	0.688	1.188737	Inhibitor/Non-substrate	Non carcinogenic

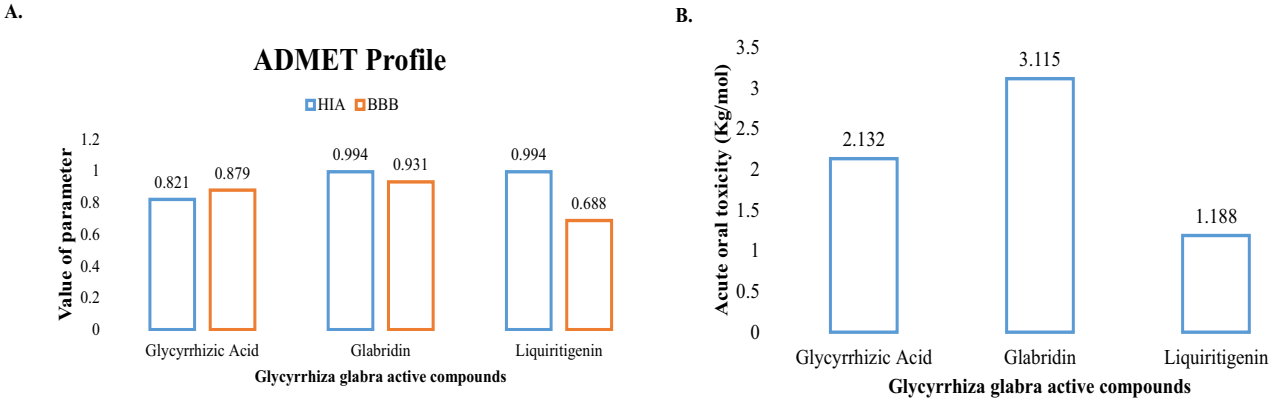

Fig. 8. A. Comparative BBB, HIA and B. Acute oral toxicity of *Gg* active compounds.

[31]. The Carcinogenic profile also shows that GA, G, and L are non-carcinogenic so it can be applied as drugs for treating COVID-19 as there would not be any bioaccumulation of compounds in the human body and these compounds would not lead to cancer in future if the patient is treated for a long duration. Acute oral toxicity was found to be higher in G followed by GA and L. It shows that L has less oral toxicity than GA which further suggests that the drugs L are not metabolized in the gastrointestinal tract before reaching the desired target. All these results have also been depicted in the form of a graph (Fig. 8 A, B and table 4).

4. Conclusion

The present studies conclude the presence of His and Cys as the conserved amino acid of M^{pro} of SARS-CoV2. Molecular docking indicated that the three active compounds of *Glycyrrhiza glabra*

namely glycyrrhizic acid, Liquiritigenin, and Glabridin successfully docked with the amino acid molecule at the catalytic site of the M^{pro} with a high negative binding affinity and formed several molecular interaction with the main protease of SARS-CoV2. They may form a complex with the M^{pro} of SARS-CoV2 causing inhibition of the catalytic activity of the main protease. His^{41} and Cys^{145} are conserved amino acids found in different types of coronavirus family and also plays a crucial role in enzyme catalysis and our docking result also showed that His^{41} and Cys^{145} are participated in the non-covalent interaction with all the three active compounds of *Glycyrrhiza glabra.* So from this study it is concluded that these active compounds exactly occupy the same location and binds these amino acid residues of the enzyme which otherwise would occupied by the natural substrates for the enzyme (M^{pro}), so these compounds can be replaced as a proposed drug for the main protease of SARS-COV2. admetSAR results show that glycyrrhizic acid would be more suitable drug candidate among the other two compounds as it is more selective, potent, non-carcinogenic, and non-tumorigenic. OSIRIS property explorer had shown Glabridin to have toxicity to the reproductive system and Liquiritigenin to be mutagenic and hence less likely be a good drug candidate than glycyrrhizic acid. The outbreak of SARS-CoV2 in December 2019 having no antiviral drug attainable for instant relief in the initial stage, This computational study may provide some promise for the designing of new antiviral drugs with least side effect and more target oriented. Our future aim would be to confirm our *in-silico* results by *in-vitro* and *in-vivo* studies.

CRediT authorship contribution statement

Vivek Srivastava: Conceptualization, Supervision. **Ankush Yadav:** Methodology, Software, Data curation, Writing - original draft. **Paratpar Sarkar:** Visualization, Investigation, Writing - review & editing.

Declaration of Competing Interest

The authors declare that they have no known competing financial interests or personal relationships that could have appeared to influence the work reported in this paper.

Acknowledgement

The authors would like to thank to Sharda University, Greater Noida, UP, India and School of Chemical and Life Sciences, Jamia Hamdard, New Delhi for writing this manuscript.

Appendix A. Supplementary data

Supplementary data to this article can be found online at https://doi.org/10.1016/j.matpr.2020.10.055.

References

[1] K. Anand, J. Ziebuhr, P. Wadhwani, J.R. Mesters, R. Hilgenfeld, Coronavirus main proteinase (3CLpro) structure: basis for design of anti-SARS drugs, Science 300 (5626) (2003) 1763–1767, https://doi.org/10.1126/science.1085658.
[2] R.M. Anderson, H. Heesterbeek, D. Klinkenberg, T.D. Hollingsworth, How will country-based mitigation measures influence the course of the COVID-19 epidemic?, The Lancet 395 (10228) (2020) 931–934, https://doiorg/10.1016/S0140-6736(20)30567-5.
[3] J. Cinatl, B. Morgenstern, G. Bauer, P. Chandra, H. Rabenau, H.W. Doerr, Glycyrrhizin, an active component of liquorice roots, and replication of SARS-associated coronavirus, The Lancet 361 (9374) (2003) 2045–2046, https://doi.org/10.1016/S0140-6736(03)13615-X.
[4] B. Gates, Responding to Covid-19 — A Once-in-a-Century Pandemic?, N Engl J Med 382 (18) (2020) 1677–1679, https://doiorg/10.1056/NEJMp2003762.
[5] Gupta, Manoj Kumar, Sarojamma Vemula, Ravindra Donde, Gayatri Gouda, Lambodar Behera, and Ramakrishna Vadde. "In-silico approaches to detect inhibitors of the human severe acute respiratory syndrome coronavirus envelope protein ion channel." Journal of Biomolecular Structure and Dynamics just-accepted (2020): 1-17. https://doi.org/10.1080/07391102.2020.1751300.
[6] S. Pandey, B. Yadav, A. Pandey, et al., Lessons from SARS-CoV-2 Pandemic: Evolution, Disease Dynamics and Future, Biology. 9 (6) (2020) 141, https://doi.org/10.3390/biology9060141.
[7] R. Hilgenfeld, From SARS to MERS: crystallographic studies on coronaviral proteases enable antiviral drug design, FEBS J 281 (18) (2014) 4085–4096, https://doi.org/10.1111/febs.12936.
[8] T. Hu, Y.u. Zhang, L. Li, K. Wang, S. Chen, J. Chen, J. Ding, H. Jiang, X.u. Shen, Two adjacent mutations on the dimer interface of SARS coronavirus 3C-like protease cause different conformational changes in crystal structure, Virology 388 (2) (2009) 324–334, https://doi.org/10.1016/j.virol.2009.03.034.
[9] C. Huang, Y. Wang, X. Li, L. Ren, J. Zhao, Y.i. Hu, L.i. Zhang, G. Fan, J. Xu, X. Gu, Z. Cheng, T. Yu, J. Xia, Y. Wei, W. Wu, X. Xie, W. Yin, H. Li, M. Liu, Y. Xiao, H. Gao, L.i. Guo, J. Xie, G. Wang, R. Jiang, Z. Gao, Q.i. Jin, J. Wang, B. Cao, Clinical features of patients infected with 2019 novel coronavirus in Wuhan, China, The Lancet 395 (10223) (2020) 497–506, https://doi.org/10.1016/S0140-6736(20)30183-5.
[10] M. Macchiagodena, M. Pagliai, P. Procacci, Identification of potential binders of the main protease 3CLpro of the COVID-19 via structure-based ligand design and molecular modeling, Chemical Physics Letters 750 (2020) 137489, https://doi.org/10.1016/j.cplett.2020.137489.
[11] A.E. Gorbalenya, E.V. Koonin, A.P. Donchenko, V.M. Blinov, Coronavirus genome: prediction of putative functional domains in the non-structural polyprotein by comparative amino acid sequence analysis, Nucl Acids Res. 17 (12) (1989) 4847–4861, https://doi.org/10.1093/nar/17.12.4847.
[12] X. Xue, H. Yu, H. Yang, et al., Structures of Two Coronavirus Main Proteases: Implications for Substrate Binding and Antiviral Drug Design, JVI 82 (5) (2008) 2515–2527, https://doi.org/10.1128/JVI.02114-07.
[13] Shanker, Arun, Divya Bhanu, and Anajani Alluri. "Analysis of Whole Genome Sequences and Homology Modelling of a 3C Like Peptidase and a Non-Structural Protein of the Novel Coronavirus COVID-19 Shows Protein Ligand Interaction with an Aza-Peptide and a Noncovalent Lead Inhibitor with Possible Antiviral Properties." (2020).
[14] Thiel, Volker, Konstantin A. Ivanov, Akos Putics, Tobias Hertzig, Barbara Schelle, Sonja Bayer, Benedikt Weißbrich et al. "Mechanisms and enzymes involved in SARS coronavirus genome expression." Journal of General Virology 84, no. 9 (2003): 2305-2315.
[15] S. Ullrich, C. Nitsche, The SARS-CoV-2 main protease as drug target, Bioorganic & Medicinal Chemistry Letters 30 (17) (2020), https://doi.org/10.1016/j.bmcl.2020.127377 127377.
[16] R. Yoshino, N. Yasuo, M. Sekijima, Identification of key interactions between SARS-CoV-2 main protease and inhibitor drug candidates, Sci Rep 10 (1) (2020) 12493, https://doi.org/10.1038/s41598-020-69337-9.
[17] R. Pompei, A. Pani, O. Flore, M.A. Marcialis, B. Loddo, Antiviral activity of glycyrrhizic acid, Experientia 36 (3) (1980) 304.
[18] R. Pompei, O. Flore, M.A. Marccialis, A. Pani, B. Loddo, Glycyrrhizic acid inhibits virus growth and inactivates virus particles, Nature 281 (5733) (1979) 689–690, https://doi.org/10.1038/281689a0.
[19] L. Wang, R. Yang, B. Yuan, Y. Liu, C. Liu, The antiviral and antimicrobial activities of licorice, a widely-used Chinese herb, Acta Pharmaceutica Sinica B 5 (4) (2015) 310–315, https://doi.org/10.1016/j.apsb.2015.05.005.
[20] V. Sharma, A. Katiyar, R.C. Agarwal, Glycyrrhiza glabra: Chemistry and Pharmacological Activity, in: J.-M. Mérillon, K.G. Ramawat (Eds.), Sweeteners, Reference Series in Phytochemistry, Springer International Publishing, 2018, pp. 87–100, https://doi.org/10.1007/978-3-319-27027-2_21.
[21] E. de Castro, C.J.A. Sigrist, A. Gattiker, V. Bulliard, P.S. Langendijk-Genevaux, E. Gasteiger, A. Bairoch, N. Hulo, ScanProsite: detection of PROSITE signature matches and ProRule-associated functional and structural residues in proteins, Nucleic Acids Research 34 (Web Server) (2006) W362–W365, https://doi.org/10.1093/nar/gkl124.
[22] S. Lu, J. Wang, F. Chitsaz, et al., CDD/SPARCLE: the conserved domain database in 2020, Nucleic Acids Research. 48 (D1) (2020) D265–D268, https://doi.org/10.1093/nar/gkz991.
[23] B.J. Mylliemngap, A. Borthakur, D. Velmurugan, A. Bhattacharjee, Insilico analysis and molecular docking of resuscitation promoting factor B (RpfB) protein of Mycobacterium tuberculosis, Bioinformation 8 (14) (2012) 646–651, https://doi.org/10.6026/97320630008646.
[24] R. Yu, L. Chen, R. Lan, R. Shen, P. Li, Computational screening of antagonist against the SARS-CoV-2 (COVID-19) coronavirus by molecular docking, International Journal of Antimicrobial Agents 56 (2) (2020) 106012, https://doi.org/10.1016/j.ijantimicag.2020.106012.
[25] L. Zhang, D. Lin, X. Sun, et al., Crystal structure of SARS-CoV-2 main protease provides a basis for design of improved α-ketoamide inhibitors, Science 368 (2020) eabb3405, https://doi.org/10.1126/science.abb3405.
[26] J. Blake, Chemoinformatics – predicting the physicochemical properties of "drug-like" molecules, Current Opinion in Biotechnology 11 (1) (2000) 104–107, https://doi.org/10.1016/S0958-1669(99)00062-2.
[27] D. Chanda, J. Prieto-Lloret, A. Singh, et al., Glabridin-induced vasorelaxation: Evidence for a role of BKCa channels and cyclic GMP, Life Sciences. 165 (2016) 26–34, https://doi.org/10.1016/j.lfs.2016.09.018.

[28] C. Simmler, G.F. Pauli, S.-N. Chen, Phytochemistry and biological properties of glabridin, Fitoterapia 90 (2013) 160–184, https://doi.org/10.1016/j.fitote.2013.07.003.
[29] M. Ramalingam, H. Kim, Y. Lee, Y-.I. Lee, Phytochemical and Pharmacological Role of Liquiritigenin and Isoliquiritigenin From Radix Glycyrrhizae in Human Health and Disease Models, Front Aging Neurosci. 10 (2018) 348, https://doi.org/10.3389/fnagi.2018.00348.
[30] O. Trott, A.J. Olson, AutoDock Vina: improving the speed and accuracy of docking with a new scoring function, efficient optimization and multithreading, J Comput Chem. 31 (2) (2010) 455–461, https://doi.org/10.1002/jcc.21334.
[31] F. Cheng, W. Li, Y. Zhou, J. Shen, Z. Wu, G. Liu, P.W. Lee, Y. Tang, admetSAR: A Comprehensive Source and Free Tool for Assessment of Chemical ADMET Properties, J. Chem. Inf. Model. 52 (11) (2012) 3099–3105, https://doi.org/10.1021/ci300367a.
[32] R. Daneman, A. Prat, The blood-brain barrier, Cold Spring Harb Perspect Biol. 7 (1) (2015), https://doi.org/10.1101/cshperspect.a020412 a020412.
[33] M. Elmeliegy, M. Vourvahis, C. Guo, D.D. Wang, Effect of P-glycoprotein (P-gp) Inducers on Exposure of P-gp Substrates: Review of Clinical Drug-Drug Interaction Studies, Clin Pharmacokinet 59 (6) (2020) 699–714, https://doi.org/10.1007/s40262-020-00867-1.
[34] A. Finch, P. Pillans, P-glycoprotein and its role in drug-drug interactions, Aust Prescr. 37 (4) (2014) 137–139, https://doi.org/10.18773/austprescr.2014.050.
[35] D. Mothay, K.V. Ramesh, Binding site analysis of potential protease inhibitors of COVID-19 using AutoDock, Virus Dis. 31 (2) (2020) 194–199, https://doi.org/10.1007/s13337-020-00585-z.
[36] Y. Kumar, H. Singh, C.N. Patel, In silico prediction of potential inhibitors for the Main protease ofSARS-CoV-2 using molecular docking and dynamics simulation based drug-repurposing, Journal of Infection and Public Health 13 (9) (2020) 1210–1223, https://doi.org/10.1016/j.jiph.2020.06.016.